

# Phase Segregation in mixed halide perovskites- is more better?

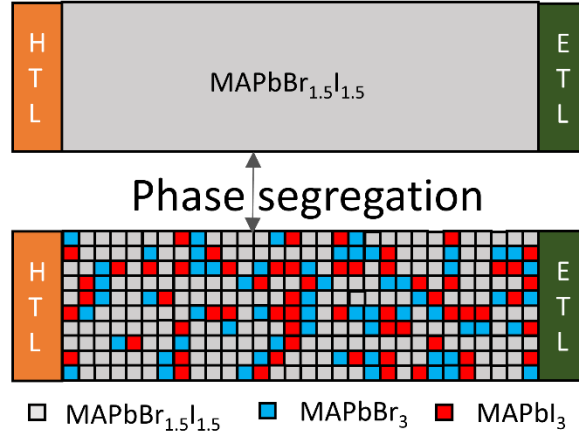
*Abhimanyu Singareddy, Uday Kiran Reddy Sadula and Pradeep R. Nair*

Department of Electrical Engineering, Indian Institute of Technology Bombay, Powai, Mumbai,  
400076, India

Email: abhir@ee.iitb.ac.in, email: prnair@ee.iitb.ac.in,

**ABSTRACT** Phase segregation is a critical phenomenon that influences the stability and performance of mixed halide perovskite based opto-electronic devices. In addition to the underlying physical mechanisms, the spatial pattern and randomness of phase segregation significantly influence performance degradation – a topic which, along with the multitude of parameter combinations, has remained too complex to address so far. Given this, with  $\text{MAPbI}_{1.5}\text{Br}_{1.5}$  as a model system, here we address the influence of critical factors like the spatial randomness of phase segregation, influence of ion migration, and the effect of increased non radiative recombination at material interfaces. Interestingly, our analytical model and detailed statistical simulations indicate a unique trend - while the device performance degrades with initial phase segregation, curiously, it recovers significantly during the later stages. Indeed, our quantitative and predictive estimates are broadly applicable to systems which undergo phase segregation and have interesting implications to perovskite based optoelectronic devices – from stability concerns to engineering approaches that attempt to arrest phase segregation.

## TOC GRAPHICS



## I. INTRODUCTION

Perovskites has evoked tremendous research interest due to interesting applications in photovoltaics<sup>1</sup>, memristors<sup>2</sup>, photodetectors<sup>3</sup>, Light Emitting Diodes<sup>4</sup>, Tandem solar cells<sup>5</sup>, etc. While bandgap tunability (through alloying different anions or cations or both)<sup>6–10</sup> is central to most such applications, phase segregation is a major concern. For example, the material  $\text{MAPbBr}_x\text{I}_{1-x}$  is unstable under various conditions and phase segregates into iodide and bromide rich domains<sup>11–13</sup> (note that, as per convention<sup>14,15</sup>, the term iodide represents  $\text{MAPbI}_3$  (Methylammonium Lead Iodide) while bromide represents  $\text{MAPbBr}_3$  (Methylammonium Lead Bromide) for the rest of this manuscript). This phenomenon is corroborated through optical measurements<sup>11,12</sup>, where two distinct Photoluminescence (PL) peaks corresponding to iodide and bromide rich domains were observed. These two domains have different generation rates according to their absorption spectra. Literature also reports photo induced phase segregation<sup>16</sup>, and electric

bias induced phase segregation<sup>17</sup> in mixed perovskite structures. Interestingly, some reports indicate a reversal of phase segregation under dark conditions, although the time taken for recovery depends on light soaking conditions.<sup>11,18,19</sup> Given the prevalence of this phenomena and its broad appeal, a few questions are of natural interest to the community – (a) What causes phase segregation? (b) What is the eventual impact of phase segregation? (c) Is it possible to arrest phase segregation? Many reports and several models tried to explain the cause of phase segregation (i.e., item a) by attributing it to the defects from halide ion vacancies which leads to the iodide and bromide rich segregated domains.<sup>20,21</sup> Alloying with a small amount of chlorine<sup>22</sup> to the mixed halide perovskite and oxygen passivation<sup>23</sup> are reported to reduce the extent of phase segregation (i.e., item c). But the exact effect of phase segregation on performance metrics of a solar cell still remains elusive (i.e., item b) – even though it is the most critical system level concern. There are no models in literature which has done the statistical simulations. In this manuscript, we address this aspect through predictive models and detailed statistical simulations. Our results, surprisingly, indicate that the device performance, although severely affected initially, in fact improves with more phase segregation. Indeed, the more the better! – albeit with significant statistical fluctuations and dependence on material parameters, most crucial among them being the increased non-radiative recombination at material or domain interfaces.

TOC figure provides the schematic of pristine device structure (PIN solar cell<sup>24</sup>) which consist of Electron Transport Layer (ETL), Active layer, and Hole Transport Layer (HTL). ETL and HTL have their conventional definition and energy level alignments<sup>25</sup> (see Fig. 1a). For the pristine device, mixed halide perovskite ( $\text{MAPbBr}_{1.5}\text{I}_{1.5}$ ) is the active layer. The figure provided in the abstract is a representation of the device at some stage of phase segregation (with randomly chosen locations for bromide and iodide domains). Here, for ease of analysis, we assume that the phase

segregation can be treated as a transformation of a single material system (i.e., MAPbBr<sub>1.5</sub>I<sub>1.5</sub>) into a complex spatial pattern which involves three different materials (although, phase segregation need not result in generation of such pure domains<sup>12</sup>). As such the material and electronic properties of the three different types of domains could be different (along with the ETL and HTL properties). Further, the presence of ion migration could significantly influence the electrostatics and hence the device performance. This could result in a plethora of parameter combinations and a detailed study could be a daunting task - not just to simulate but also to understand, assimilate, and convey the insights as well – precisely what we aim to achieve in this manuscript! The strategy is as follows: (a) we first explore the critical influence of spatial pattern or geometry of phase segregation (at low ion concentrations). To this end, we assume that the three perovskites under consideration differ only in their band gaps (and hence photo-carrier generation rates) with corresponding energy level alignments shown in Fig. 1a. (b) Second, we consider the combined influence of ion migration and phase segregation (i.e., this is a case of high ion density), and (c) finally, the critical effect of the combination of the phase segregation, high ion density, and the phase segregation dependent carrier lifetime degradation (due to a variety of factors which include increased non-radiative recombination at the phase segregated domains and/or at the interfaces between domains). Such a hierarchical approach of models of increasing complexity indeed helps to quantitatively estimate the influence of phase segregation in mixed halide perovskite devices. Note that here we address the influence of abovementioned phenomena on the steady state efficiency of perovskite solar cells. Transient effects like hysteresis, while interesting, could be taken up later.

Detailed information regarding methodology and parameters used in simulations are provided in Section I, Suppl. Info.

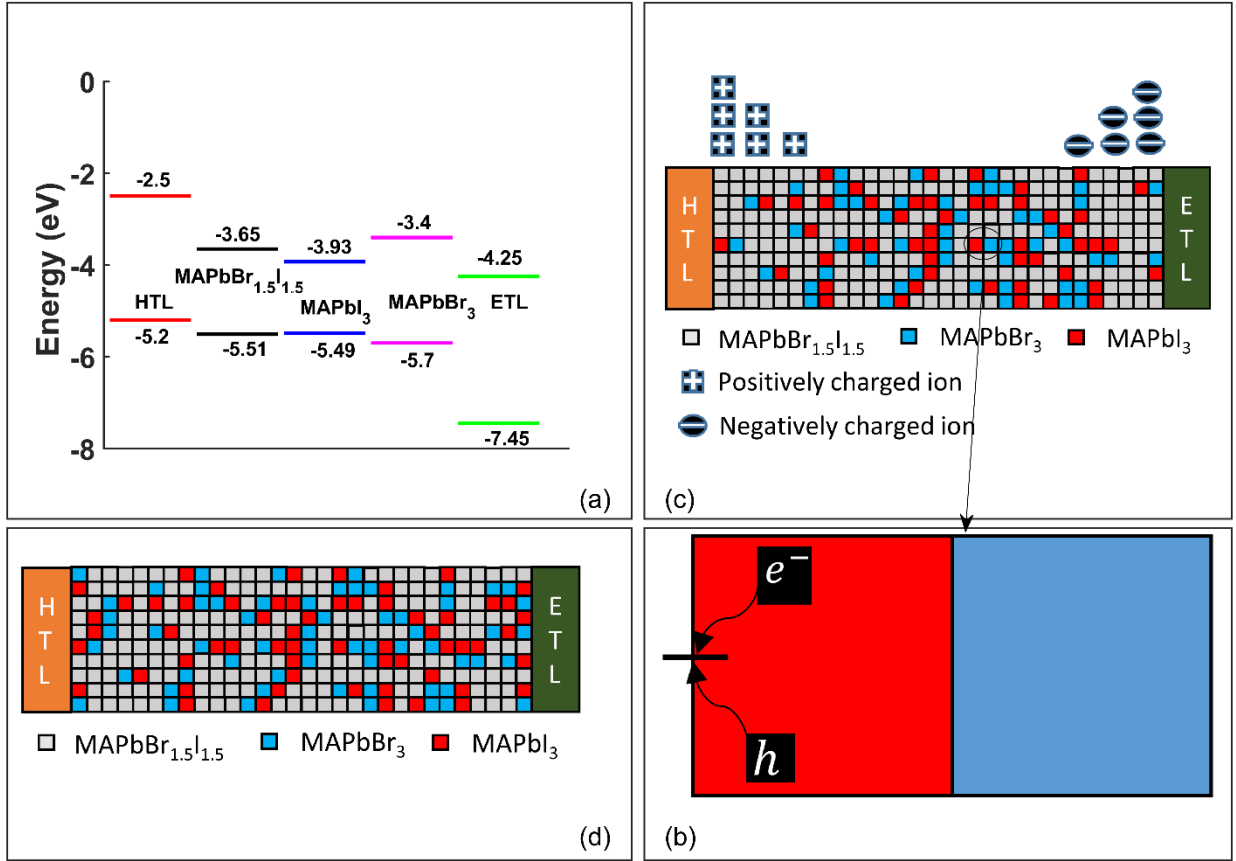


**Figure 1:** A 2D model system to study the effect of phase segregation in mixed halide perovskite solar cells. (a) Energy levels of different materials<sup>25</sup>. The HTL properties correspond to Spiro-OMeTAD and ETL properties correspond to TiO<sub>2</sub>. (b) Schematic of the model used to study the effect of spatial randomness in the phase segregated device (low ion density case). (c) Schematic used to investigate ion migration effects in a phase segregated device (high ion density case). (d) Schematic shows the increased non radiative recombination due to the traps present at the boundary of iodide domain along with the effect of ion migration in a phase segregated device.

## II. PREDICTIVE MODEL

Before we discuss the detailed simulation results, let us first attempt to arrive at analytical estimates for the performance metrics. Even with such a complex network of domains with heterojunctions, surprisingly, a few aspects related to phase segregation can be anticipated based on simple facts

related to band level alignments and carrier transport. Note that the domains could be either iodide or bromide or mixed halide. As the energy level alignments indicate (see Fig. 1a), bromide domains are not energetically favorable for electrons. As a result, the electrons are expected to avoid the bromide domains and mostly flow through iodide or mixed halide domains. At low phase segregations, almost all paths from ETL could end up in HTL as the bromide domains could be a few and isolated. At very large phase segregations, the bromide domains could introduce significant impediment to photo-carrier collection. In addition, the efficiency of carrier collection is expected to depend on the internal electric field and hence the applied bias. Curiously, this could be significantly influenced by the presence of ions in the photo-active layer. Accordingly, any predictive model needs to account for the influence of carrier transport and ion influenced electrostatics in the perovskite active layer- as accomplished in this section.

(a) **Hypothesis on  $J_{SC}$ :** Using parameters from Shockley-Queisser analysis<sup>26</sup>, uniform optical absorption, and an optical loss<sup>27</sup> of 20%, we have  $G_I = 4.53 \times 10^{21} \text{ cm}^{-3}\text{s}^{-1}$ ,  $G_M = 2.98 \times 10^{21} \text{ cm}^{-3}\text{s}^{-1}$ , and  $G_B = 1.48 \times 10^{21} \text{ cm}^{-3}\text{s}^{-1}$  as the photo-carrier generation rates for the iodide, mixed halide, and bromide domains, respectively (see Section I of Suppl. Info). Let  $N_I$ ,  $N_M$ , and  $N_B$  denote the number of domains of iodide, mixed halide, and bromide, respectively. If we assume domains to have the same volume, then the level of phase segregation ( $\vartheta$ ) can be defined as

$$\vartheta = \frac{N_I + N_B}{N_I + N_M + N_B}. \quad (1)$$

Assumption of volume conservation during phase segregation leads to  $N_I + N_M + N_B = N_T$  where  $N_T$  is a constant (300 in our simulations) and  $N_I = N_B$ . The collection efficiency of photo-

generated carriers depends on the density of ions present in the perovskite active layer. In this case, two limiting scenarios could be easily identified:

**(i) Low ion density:** In this case, due to negligible amount of charge in the perovskite active region, the device will behave like a classical PIN structure. The simulated E-B diagram is shown as inset in Fig. 2a. Accordingly, the dominant carrier collection mechanism is field assisted drift. For an assumed carrier mobility ( $\mu$ ) of  $2 \text{ cm}^2/\text{Vs}$ , effective carrier lifetime ( $\tau_{eff}$ ) of 100 ns, a built-in potential of 0.784 V, and active layer thickness of 300nm, the drift collection length ( $\mu\tau_{eff}E$ ,  $E$  is the electric field) at short circuit conditions is  $\sim 52 \text{ }\mu\text{m}$ . Since the drift collection length is much larger than the device thickness and neglecting the effect of potential barriers induced by bromide domains (see Fig. 1a) we have (details provided in Section II, Suppl. Info).

$$J_{SC} = q \frac{(N_I G_I + N_M G_M + N_B G_B)}{N_T} l, \quad (2)$$

where  $l$  is the thickness of active layer (300nm in our case,). For the specific problem under consideration, we note that  $G_M \sim (G_I + G_B)/2$ . Accordingly, eq (2) indicates that

$$J_{SC} \sim q G_M l, \quad (3)$$

and hence the  $J_{SC}$  will be independent of phase segregation.

**(ii) High Ion density:** In this case, the ions screen the  $V_{bi}$  and the negligible electric field is present in the perovskite active layer even during short circuit conditions (the E-B diagrams are provided in Fig. 3a). Consequently, photo-carrier collection is dominated by diffusion and the corresponding collection length is given as  $\sqrt{D\tau_{eff}}$ . For similar set of parameters, the diffusion collection length is about 700nm, which is larger (but not significantly larger) than the active layer thickness of

300nm. Hence, we expect a weak dependence of photo-carrier collection and hence the  $J_{SC}$  on phase-segregation.

The above arguments indicate that regardless of the presence of ions in the active layer, the  $J_{SC}$  is expected to show only a very weak dependence on phase segregation. This is a consequence of the fact that both the drift as well as diffusion collection lengths under short circuit conditions are larger than the active layer thickness. On the other hand, if the lifetime of carriers reduces to 1ns, the drift and diffusion collection lengths are 520nm and 70nm, respectively. Accordingly, our model predicts significant reduction in  $J_{SC}$  in the presence of lifetime degradation and high ion densities. We remark that the model predictions on  $J_{SC}$  also depends directly on the band gaps of various phases and could vary if one were to start with a different mixed halide perovskite other than the one under consideration (in such a case only  $G_M$  changes with no change in  $G_I$  or  $G_B$ ).

**(b) Predictions for  $V_{oc}$ :** The  $V_{oc}$  of an isolated intrinsic domain is given as  $V_{oc} = \frac{2kT}{q} \ln \left( \frac{G\tau_{eff}}{n_i} \right)$  where  $G$ ,  $n_i$ , and  $\tau_{eff}$  are the generation rate, intrinsic concentration, and the effective carrier lifetime in the active layer, respectively (derivation in suppl. Info.). Accordingly, the  $V_{oc}$  of mixed halide, bromide, and iodide domains are  $V_{oc,MX} = 1.36V$ ,  $V_{oc,B} = 1.73V$ , and  $V_{oc,I} = 1.08V$ , respectively (see Section III, suppl. Info for details). Naturally, the  $V_{oc}$  of a device without any phase segregation will be 1.36V. For 100% phase segregation, only iodide and bromide domains will be left as active components. Here, one may expect significant contribution by bromide domains to  $V_{oc}$ . However, such a strong influence of bromide domains is unlikely due to the fact that the iodide domains act as potential well for electrons (see energy level alignment in Fig. 1a). Accordingly, carrier accumulation is expected in iodide domains and the recombination in the same domains could dictate the  $V_{oc}$ . Applying the principle of detailed balance, we have



$$N_T G_M = \frac{N_I \Delta n}{\tau_{eff}}, \quad (4)$$

where the LHS denotes the net photo-carrier generation in the device while the RHS is the net carrier recombination in the iodide domains. Here  $\Delta n$  denotes the excess carrier density and  $\tau_{eff}$  denotes the effective carrier lifetime. As iodide domains act as potential wells for carriers, recombination in other domains is ignored in this analysis (validity of the same will be evident once we discuss numerical simulation results). Under such conditions, the  $V_{oc}$  is nothing but the split in quasi-Fermi levels in the intrinsic iodide domains. Accordingly, for  $\vartheta \neq 0$ , Eqs. (1)-(4) lead us to

$$V_{oc}(x) = \frac{2kT}{q} \ln \left( \frac{2G_M \tau_{eff}}{\vartheta n_{il}} \right), \quad (5)$$

where  $n_{il}$  is the intrinsic concentration in the iodide domain. Eq. (5) predicts that the  $V_{oc}$  varies as  $\ln(\vartheta)$  and hence is not expected to be strongly dependent on phase segregation (except when  $\vartheta$  is small). We note that the predicted  $V_{oc}$  dependence on phase segregation in mixed halide perovskites (i.e., Eq. (5)) is distinctly different from the  $V_{oc}$  scaling trends observed in multi-component organic solar cells<sup>28,29</sup> (where the influence of all components are explicit due to the inherent nature of non-geminate recombination at interfaces). Although only a weak dependence is predicted by eq. (5), some variations in  $V_{oc}$  are expected due to the spatial pattern of phase segregation and the influence of band alignment of the active layer components with the contact layers (see Fig. 1a). Further, it is interesting to observe that the prediction for  $V_{oc}$  (i.e., eq. (5)) is valid irrespective of the ion density in the active layer. This is due to the fact that under  $V_{oc}$  conditions, regardless of the ion density, negligible electric field is present in the perovskite active layer and hence detailed balance analysis is expected to hold.

(c) **Hypothesis on Fill Factor (FF):** For the PIN structures under consideration, the maximum power-point happens at conditions where the internal electric field could be very small. Accordingly, the carrier collection at such conditions will be dominated by diffusion. Depending on the extent of phase segregation, the carrier extraction from isolated iodide domains might be difficult at such conditions and hence this could lead to significant FF dependence on the spatial pattern of phase segregation. As the level of phase segregation increases, we expect more and more such isolated iodide domains. Large clusters and interconnected pathways (very similar to percolation phenomena<sup>30</sup>) could emerge for large phase-segregation. Under such conditions, we expect the FF to decrease first with phase segregation (with less statistical fluctuations) and then as the iodide domains form large clusters or pathways the FF is expected to increase (with large statistical fluctuations as some such pathways might lead to much better carrier collection than others). As with the  $V_{oc}$ , this prediction is expected to hold regardless of the density of ions in the active layer as carrier collection is significantly influenced by diffusion at  $V_{mpp}$  (maximum power point) conditions.

(d) **Efficiency:** Summing up, regardless of these complexities, we expect  $J_{sc}$  to be fairly independent of phase segregation (for all cases other than simultaneous occurrence of large ion density and significant lifetime degradation). The  $V_{oc}$  could show a decreasing, although not very dramatic, trend with phase segregation. The FF could first decrease and then increase with phase segregation. Overall, the efficiency is then expected to follow the trends of  $J_{sc}$  and FF. It is expected to reach a minimum and then increase with further phase segregation – along with significant fluctuations. For the specific cases of lifetime degradation coupled with large ion densities, we expect a decrease in efficiency with phase-segregation. These predictions will be now compared against detailed numerical simulations.

### III. SIMULATIONS

Numerical simulation of a multi-heterojunction device with random domains is a computationally challenging job, and the following simulation methodology is adopted: The perovskite active layer is assumed to consist of several individual domains, where the material properties of each domain can be uniquely defined. Self-consistent numerical solution of Poisson and Carrier continuity equations<sup>31</sup> in two dimensions and steady state conditions is used to explore the effect of phase segregation with explicit consideration of heterojunctions between various domains. The presence of ions is also self-consistently accounted through the Poisson's equation. Here the 300nm thick perovskite layer (see Fig. S1, supply info.) is divided into  $N_T = 300$  domains each of  $10nm \times 10nm$  size<sup>32</sup>. Upon illumination, a certain fraction of the photo-active material  $MAPbBr_{1.5}I_{1.5}$  gets phase segregated into  $MAPbI_3$  and  $MAPbBr_3$  domains. For ease of analysis, we consider only the case of complete phase segregation with an implicit assumption of volume conservation – i.e., two  $MAPbBr_{1.5}I_{1.5}$  domains phase segregate into two domains - one  $MAPbI_3$  and one  $MAPbBr_3$  (in reality, the domains need not be purely iodide or bromide<sup>11</sup>. However, such a scenario is beyond the scope of this submission and could be handled with an effective set of material parameters). For a given volume fraction of such phase segregation, first the corresponding bromide domains are placed randomly, then iodide domains are identified within the neighborhood of respective bromide domains. To gain insights into the statistics and influence of spatial pattern of Br/I domains on solar cell performance, different random manifestations were simulated (20 different spatial distributions) for each volume fraction of phase segregation.

As discussed in Section I, the combinations of material parameters and spatial patterns of phase-segregation is too large to attempt an exhaustive simulation study. Still, aided with the insights from analytical model (Section II), we address the following effects – (a) influence of geometry or spatial pattern of phase segregation, (b) Combined effect of ion migration and phase segregation, and (c) critical influence of lifetime degradation in conjunction with ion migration. We did explore a few other relevant aspects like influence of band alignment and mobility variation, which were not found to be as influential as those listed above and hence will be communicated separately. As a calibration, we first performed simulations of PIN structures with only one active material. These characteristics are as expected, and the  $V_{oc}$  values compare very well with the analytical predictions (results shared in Section IV of Suppl. Info). Below, we discuss simulation results related to phase segregation:

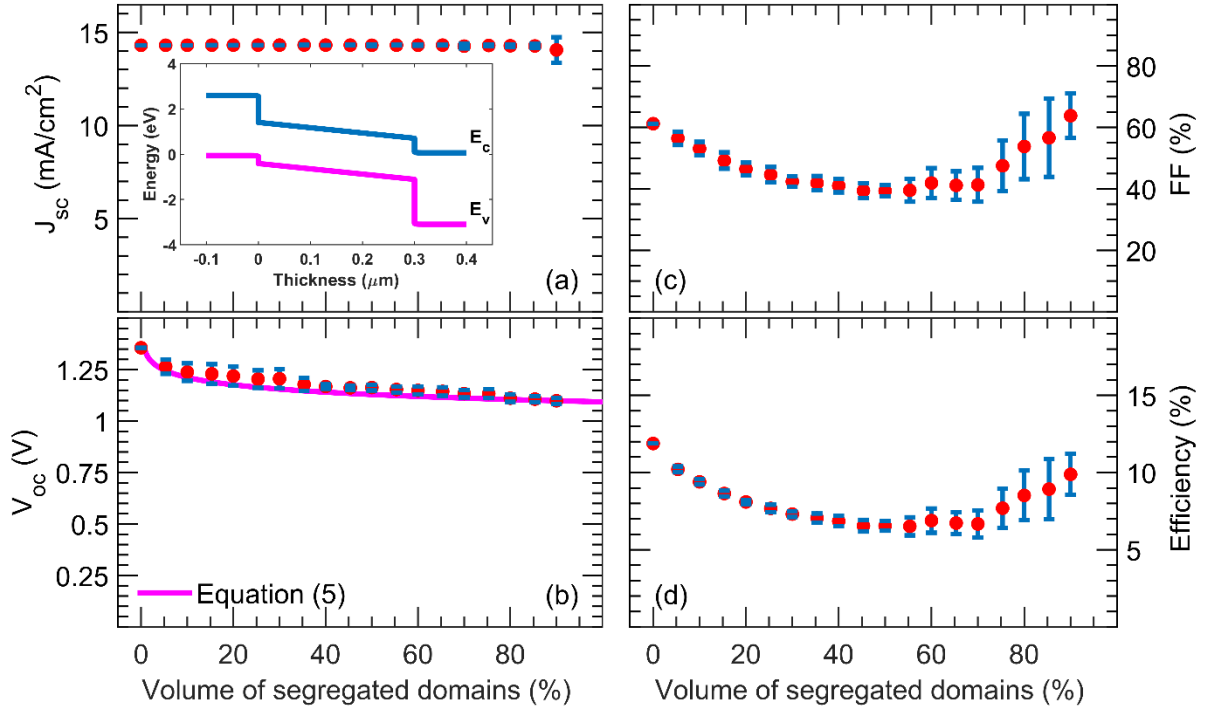


**Figure 2.** Effect of phase segregation on the performance parameters of a solar cell. (a) Short circuit current ( $J_{sc}$ ), Inset figure represents the equilibrium band diagram of the mixed halide perovskite before segregation, (b) Open circuit voltage ( $V_{oc}$ ), (c) Fill Factor (FF), and (d) efficiency. Note that all plots show the mean and standard deviation of the normalized parameters. Although the simulations accounted for SRH, radiative and Auger recombination in perovskite active layer, Eq. (5) was plotted with only the SRH lifetime as it dominates the recombination. Other details are provided in supplementary information.

**(a) Geometry of Phase segregation:** We first assume a set of parameters (provided in suppl.info) and then explore the influence of the spatial pattern of phase segregation on the solar cell performance. The statistics of such simulations for various levels of phase segregation is provided in Fig. 2. For each volume fraction of phase segregation, we performed numerical simulations of 20 different spatial configurations (i.e., ~360 simulations were performed to generate this figure) and the mean and variance of each data set is plotted. The corresponding scatter data is provided in Section V, Suppl. Info. Interestingly, broad features of these results are in accordance with the analytical model, as listed below:

(a) The  $J_{sc}$  is almost independent of phase segregation (shown in Fig. 2a) as the carrier collection length is much larger than device thickness, as predicted in the previous section. We note that reduction in  $J_{sc}$  is seen in some configurations associated with large fraction of phase segregation. In such cases, we find that the bromide domains create significant obstruction to current collection.

(b)  $V_{oc}$  trends (see Fig. 2b) are also reasonably well anticipated by the analytical model (Eq. 5). This is not a surprise as eq. (5) was derived using the principle of detailed balance. Further, as expected, the fluctuations in  $V_{oc}$  decrease as iodide domains increase in number.

(c) Our analytical model accurately predicts the FF trends (see Fig. 2c) – both the mean and the variation. FF degrades initially and then improves with an increase in phase segregation. Further, we observe that for large phase segregation, the FF could be even better than that of the pristine device – which is a direct consequence of the influence of contact layer properties. For such cases, carrier collection is mainly through interconnected iodide domains in direct contact with transport layers. As demonstrated in Section IV of Suppl. Info, PIN schemes with iodide perovskite as the only active layer component results in much better FF as compared to devices with either bromide or mixed halides.

(d) Part (d) of Fig. 2 indicates that phase-segregation leads to an initial degradation of efficiency and then a recovery with significant variations – which was also predicted by our analytical model. For low phase segregation volumes, the iodide clusters are still isolated which results in increased recombination and hence decrease in efficiency. The performance recovers significantly for larger volume fractions of phase segregation. This improvement is contributed mainly by the emergence of carrier collection pathways where iodide domains are interconnected which results in better carrier collection and hence an increase in FF.

(e) Even though the performance recovers for larger values of phase segregation, the associated variation also becomes quite significant. This indicates that there could be significant device-device variability for larger phase segregations.

**(b) Influence of Ion migration:** Perovskite materials are often plagued by the migration of ions which leads to degradation of material,<sup>33</sup> in turn significantly affects the performance. This migration is due to the low activation energies<sup>34</sup> of the ions in the lattice which can be easily overthrown with external factors such as external bias, light, heat etc., The charged species i.e the ions or the vacancies left by them could be either positive or negatively charged. These ions when driven by the voltage could accumulate at the interface and hamper the performance of the device. In order to study the effects of migration of ions in the phase segregated device, we have assumed an ion density  $N_I = 10^{18} \text{ cm}^{-3}$ . These ions screen the inbuilt electric field and accumulate at the respective interfaces and (see Fig. 3a). This results in a flat band condition which changes the carrier transport from drift to diffusion-based mechanism. Indeed, the accumulated ionic charge varies as a function of applied bias and is shown in Fig. 3b, where the term dipole charge denotes the net ionic charge over half the width of perovskite active layer  $(\int_0^{l/2} N_I(x) dx)$ . Minor deviations are observed in  $J_{sc}$  with respect to the device without ions (which is expected as the carrier collection is now diffusion dominated), while the  $V_{oc}$  trends are almost same (see Fig. S4a of suppl info.). We note that these trends are in accordance with the model predictions. Even in the presence of ions, we find that efficiency variation in a phase segregated device follows a universal trend – an initial decrease with small fluctuations followed by a recovery with large fluctuations.

**(c) Influence of lifetime degradation:** - Many reports suggested that the non-radiative recombination increases in a device after phase segregation []. It could be due to deep traps at the boundaries or from the defects due to segregation in the device. Such lifetime degradation due to trap states at domain interfaces (or high recombination velocity) or low lifetime in domains could be conveniently modeled using the methodology described in Suppl. Mat. A limiting case estimate for such domain interface recombination influenced lifetime is given as  $\tau_{eff} \sim d/4S$ , where  $d$  is the size of domains, and  $S$  is the surface recombination velocity. As an illustration, here we consider an interface recombination velocity of  $S = 250 \text{ cm/s}$ , which results in an effective carrier lifetime of  $1 \text{ ns}$  in iodide domains. The effect of such lifetime degradation is explored in the presence of ion migration (see Fig. 3c, d).

As discussed in the previous section, migration of ions flattens the bands which makes diffusion a dominant mode of transport. Any reduction in the lifetime (say, due to recombination at domain interfaces) will further reduce the overall diffusion length of carriers. For  $S = 250 \text{ cm/s}$  or an effective lifetime of  $1 \text{ ns}$  in iodide domains, we have  $l_{diff} = \sqrt{D\tau_{eff}}$  which is around  $72 \text{ nm}$ . This length is shorter than the thickness of the device. So, as the number of iodide domains increase, the carrier recombination increases which results in a drastic reduction in  $J_{sc}$  with respect to the volume of segregated domains (see Fig. 3c). The trends for  $V_{oc}$  and FF are provided in the supplementary info. The variations in  $J_{sc}$  is reflected in efficiency (see Fig. 3d) which indicates that the recovery in efficiency at higher segregation volumes is significantly hampered. Further as  $\tau_{eff} \sim d/4S$ , even modest amounts of interface degradation results in significant reduction in effective carrier lifetime. For example, the carrier lifetime degrades by an order of magnitude (i.e., from  $100 \text{ ns}$  to  $10 \text{ ns}$ ) even with  $S = 25 \text{ cm/s}$ . With typical carrier capture coefficients in the range  $10^{-7}$  to  $10^{-10} \text{ cm}^3/\text{s}$ , the above correspond to an interface state trap density ( $D_{it}$ ) of around



$5 \times 10^8$  to  $5 \times 10^{11} \text{ cm}^{-2}$  (derivation in suppl. Info.). This is a result of immense importance as there is a strong correlation between domain size, interface state density and hence the effective lifetime. As the domain sizes are small (of the order of  $10 \text{ nm}$ ), such low values of interface state density (equivalently S) lead to low effective lifetimes. Hence it is important to either arrest phase segregation or passivate the interfaces – which are essential towards long term stability of such devices.

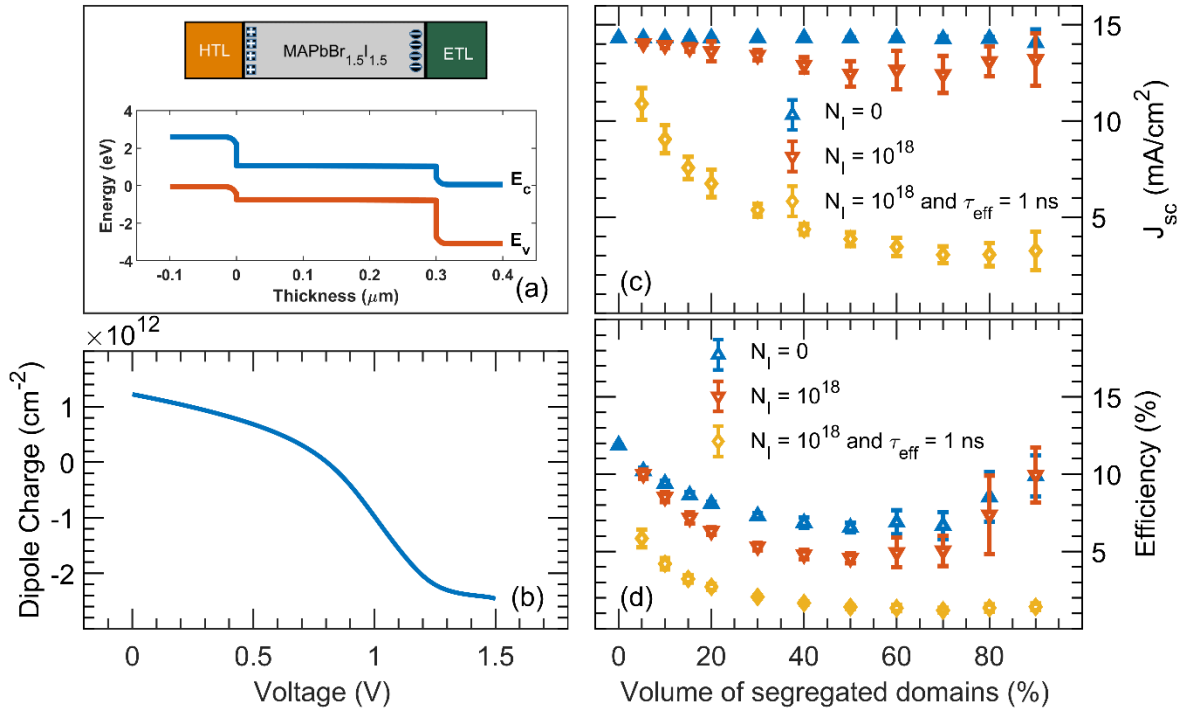


**Figure 3:** Influence of ions and the lifetime degradation in iodine domain on the phase segregated device. (a) Schematic of the device with ions accumulated at the interface due to the inbuilt electric field in a PIN device (see inset of Fig. 2a) before segregation and the corresponding equilibrium band diagram, (b) Variation of ion density (Dipole charge) at the interfaces due to the voltage sweep, (c, d) Comparison of  $J_{sc}$  and efficiency in three different scenarios, 1) A simple phase segregated device, 2) Inclusion of ions (ion density  $N_I = 10^{18} \text{ cm}^{-3}$ ) in the phase segregated device, and 3) Influence of lifetime degradation in iodide domain ( $\tau_{iodide} = 1 \text{ ns}$ ) in a ions dominated segregated device. Note that c, d plots show the mean and standard deviation of the normalized efficiencies. For each volume fraction, at least 20 different random spatial configurations of phase segregation were simulated to obtain the statistics.

#### IV. Discussions

Here we first compare the trends from simulations with available experimental data. Note that we addressed phase-segregation as transformation of a single component system into a three-component system. As such the conclusions should be broadly applicable to not just mixed halide perovskites but to other systems like quaternary system<sup>16,17,35,36</sup> which also exhibit phase segregation. While there are many reports on material characterization of systems undergoing phase segregation,<sup>11,18,19,21,37–39</sup> only a few studies have reported the effect of phase segregation on solar cells characteristics<sup>17,36,40–42</sup> – that too for individual devices and not any statistical study. In addition, simple comparisons with experimental results are not always quantitative due to the measurement delays and the uncertainty associated with the extent of phase segregation (i.e., the initial measurement might correspond to an unknown  $\vartheta \neq 0$ ). Still, degradation in  $V_{oc}$ , FF and efficiency are commonly reported<sup>13,17,40</sup> in literature and are in accordance with the results presented here. Observed degradation<sup>40,42</sup> in  $J_{sc}$  could arise due to a degradation in effective carrier lifetime or due to ion migration which can result in diffusion dominant carrier transport mechanism or combination of both. Curiously, an increase in  $J_{sc}$  during phase segregation was reported recently<sup>17</sup> – which is not observed that regularly. Our analysis indicates that such a  $J_{sc}$  increase, typically, would require formation of continuous paths of iodide from HTL to ETL at higher phase

segregation volumes and/or a simultaneous improvement in the carrier lifetime as well. We reserve attempts for a better quantitative analysis since the extent of initial phase segregation is unknown in any of the reported experimental results. As mentioned before, detailed experimental studies to understand statistical effects of phase segregation are yet to reported. In this context, this work is very relevant as the influence of parametric variations is clearly elucidated in terms of the geometry or spatial configuration, influence of the ion migration, and the effectiveness of carrier collection. Indeed, the insights gained from the analytical model helped us to carefully select the parameter combinations for numerical simulations (results from  $\sim 1020$  simulations are reported in this submission) which allowed us to explore and understand the complexities associated with phase-segregation in a structured way.

Having explored the key features of phase segregation, let us ponder about the broader implications. Our results indicate that phase segregation, ion migration and recombination at the domain interfaces have a critical influence towards the long-time operation and stability of perovskite based devices. We found that efficiency degrades significantly even with trap states of density  $5 \times 10^8 \text{ cm}^{-2}$  at domain interfaces. Such areal densities correspond to bulk state density of around  $2 \times 10^{15} \text{ cm}^{-3}$ . Further, domain size as well as interface traps are intrinsically connected to the performance of the system. Given that the efficiency recovers, should one attempt to arrest phase segregation? The answer is evident in Fig. 2d and Fig. 3d which indicates that same efficiency could be achieved at two different levels of phase segregation. However, the level of fluctuations is much smaller for lower values of phase segregation and hence it is always better to identify schemes<sup>43</sup> which can arrest phase segregation. At the low levels, the effect of ions has a minimal effect, as it evident from the little variation seen in fig. 3d. Even at lower phase segregation levels, we need to be cautious about the degradation in effective lifetime due to the

trap states at the interface. As discussed above, even the lower values of  $S$  shows the effect of high interface recombination rates at the grain boundaries. If ignored it will have detrimental effect on the solar cell as a whole. To maximize performance, the better way is to passivate these traps. . On a related note, how would the design of tandem cells with mixed halides as top cells is going to be affected? Evidently, this is a complex task as the band gap and hence region of absorbed solar spectra could vary significantly that could render initial designs and optimizations ill suited. In this scheme also, arresting phase segregation has immense significance. Further, what might be the trends for phase-segregation with other mixed halides, say with  $\text{MAPbI}_x\text{Br}_{3-x}$ , where  $x \neq 1.5$ ? For such cases, the broad trends as discussed here should hold. We note that  $\text{MAPbI}_{1.5}\text{Br}_{1.5}$  has a band gap which resulted in net photo-carrier generation being a constant regardless of phase segregation. Although the same need not hold for other mole fractions, our analysis and simulation methodology could be easily extended to such cases (i.e., with mole fraction  $x \neq 1.5$ ).

Finally, we wish to make a passing reference on similarity between carrier transport in phase segregation with the percolation concepts. In fact, the collection of photo-generated carriers at any level of phase segregation is very similar to percolation<sup>30</sup>, except that classical percolation involves infinite potential barriers as against the finite potential barriers we encounter in halide phase segregation. Indeed, the fluctuations observed in this work are related to collection pathways and specific geometric pattern of various domains. Evidences of the influence of such percolated transport is observed in our simulations – especially in those related to the role of band level alignments. However, those results follow the broad trends discussed in this manuscript and will be communicated elsewhere. More complex 3D simulations could be provide additional interesting insights.

## V. Conclusions

To summarize, here we have provided quantitative estimates for the effect of phase segregation on mixed halide perovskite solar cells. Through a combination of analytical modeling and detailed numerical statistical simulations, we addressed the influence of critical aspects like spatial randomness, ion migration, and carrier collection efficiency. Our results indicate that while small amounts of phase segregation are indeed detrimental, performance recovers for larger values of phase segregation – a universal trend that holds over a broad range of material/electrical parameters. These trends are supported by experimental trends available in literature. Our results are of immense significance for high efficiency tandem solar cells as phase segregation could be induced by illumination and could help in the design of optimal light soaking conditions which could result in stabilized efficiency for mixed halide perovskite solar cells. Indeed, the analytical predictions, simulation methodology and insights shared in this manuscript are broadly applicable to other perovskite systems where phase segregation could be a concern. Evidently, this work could help in the design of experiments to explore the statistics of phase segregation and interface engineering to reduce the influence of the same.

### ASSOCIATED CONTENT

**Supporting Information.** Simulation methodology, Derivation for short circuit current, Detailed balance analysis for open circuit voltage, I-V characteristics of PIN solar cells and important features, Influence of geometry of spatial pattern of phase segregation Modeling the ion migration and study its effects, Modeling of interface recombination as effective lifetime.

## AUTHOR INFORMATION

Email: abhir@ee.iitb.ac.in, email: prnair@ee.iitb.ac.in,

### ORCID

Abhimanyu singareddy: 0000-0002-9408-8386

Uday kiran Reddy Sadula: 0000-0003-4473-7402

Pradeep R. Nair:0000-0001-9977-2737

### Notes

The authors declare no competing financial interest.

### ACKNOWLEDGMENT

This work was supported by Science and Engineering Research Board (SERB, project code: CRG/2019/003163), Department of Science and Technology, India. The authors would like to acknowledge CEN and NCPRE, IIT Bombay, India for computational facilities. We acknowledge the financial support of University Grants Commission (UGC), India. PRN also acknowledges Visvesvaraya Young Faculty Fellowship.

### REFERENCES

- (1) Jeon, N. J.; Na, H.; Jung, E. H.; Yang, T. Y.; Lee, Y. G.; Kim, G.; Shin, H. W.; Il Seok, S.; Lee, J.; Seo, J. A Fluorene-Terminated Hole-Transporting Material for Highly Efficient and Stable Perovskite Solar Cells. *Nat. Energy* **2018**, *3* (8), 682–689. <https://doi.org/10.1038/s41560-018-0200-6>.
- (2) Xiao, X.; Hu, J.; Tang, S.; Yan, K.; Gao, B.; Chen, H.; Zou, D. Recent Advances in Halide Perovskite Memristors: Materials, Structures, Mechanisms, and Applications. *Adv. Mater.*

- Technol.* **2020**, 5 (6), 1–29. <https://doi.org/10.1002/admt.201900914>.
- (3) Miao, J.; Zhang, F. Recent Progress on Highly Sensitive Perovskite Photodetectors. *J. Mater. Chem. C* **2019**, 7 (7), 1741–1791. <https://doi.org/10.1039/C8TC06089D>.
- (4) Zhang, Q.; Zhang, D.; Gu, L.; Tsui, K.-H.; Poddar, S.; Fu, Y.; Shu, L.; Fan, Z. Three-Dimensional Perovskite Nanophotonic Wire Array-Based Light-Emitting Diodes with Significantly Improved Efficiency and Stability. *ACS Nano* **2020**. <https://doi.org/10.1021/acsnano.9b06663>.
- (5) Bush, K. A.; Palmstrom, A. F.; Yu, Z. J.; Boccard, M.; Cheacharoen, R.; Mailoa, J. P.; McMeekin, D. P.; Hoyer, R. L. Z.; Bailie, C. D.; Leijtens, T.; Peters, I. M.; Minichetti, M. C.; Rolston, N.; Prasanna, R.; Sofia, S.; Harwood, D.; Ma, W.; Moghadam, F.; Snaith, H. J.; Buonassisi, T.; Holman, Z. C.; Bent, S. F.; McGehee, M. D. 23.6%-Efficient Monolithic Perovskite/Silicon Tandem Solar Cells With Improved Stability. *Nat. Energy* **2017**, 2 (4), 1–7. <https://doi.org/10.1038/nenergy.2017.9>.
- (6) McMeekin, D. P.; Sadoughi, G.; Rehman, W.; Eperon, G. E.; Saliba, M.; Hörantner, M. T.; Haghighirad, A.; Sakai, N.; Korte, L.; Rech, B.; Johnston, M. B.; Herz, L. M.; Snaith, H. J. A Mixed-Cation Lead Mixed-Halide Perovskite Absorber for Tandem Solar Cells. *Science* (80-. ). **2016**, 351 (6269), 151–155. <https://doi.org/10.1126/science.aad5845>.
- (7) Rosales, B. A.; Hanrahan, M. P.; Boote, B. W.; Rossini, A. J.; Smith, E. A.; Vela, J. Lead Halide Perovskites: Challenges and Opportunities in Advanced Synthesis and Spectroscopy. *ACS Energy Lett.* **2017**, 2 (4), 906–914. <https://doi.org/10.1021/acsenenergylett.6b00674>.
- (8) Noh, J. H.; Im, S. H.; Heo, J. H.; Mandal, T. N.; Seok, S. Il. Chemical Management for Colorful, Efficient, and Stable Inorganic-Organic Hybrid Nanostructured Solar Cells. *Nano*

- ett.* **2013**, *13* (4), 1764–1769. <https://doi.org/10.1021/nl400349b>.
- (9) Yi, C.; Luo, J.; Meloni, S.; Boziki, A.; Ashari-Astani, N.; Grätzel, C.; Zakeeruddin, S. M.; Röthlisberger, U.; Grätzel, M. Entropic Stabilization of Mixed A-Cation ABX<sub>3</sub> Metal Halide Perovskites for High Performance Perovskite Solar Cells. *Energy Environ. Sci.* **2016**, *9* (2), 656–662. <https://doi.org/10.1039/c5ee03255e>.
  - (10) Suarez, B.; Gonzalez-Pedro, V.; Ripolles, T. S.; Sanchez, R. S.; Otero, L.; Mora-Sero, I. Recombination Study of Combined Halides (Cl, Br, I) Perovskite Solar Cells. *J. Phys. Chem. Lett.* **2014**, *5* (10), 1628–1635. <https://doi.org/10.1021/jz5006797>.
  - (11) Hoke, E. T.; Slotcavage, D. J.; Dohner, E. R.; Bowring, A. R.; Karunadasa, H. I.; McGehee, M. D. Reversible Photo-Induced Trap Formation in Mixed-Halide Hybrid Perovskites for Photovoltaics. *Chem. Sci.* **2015**, *6* (1), 613–617. <https://doi.org/10.1039/c4sc03141e>.
  - (12) Slotcavage, D. J.; Karunadasa, H. I.; McGehee, M. D. Light-Induced Phase Segregation in Halide-Perovskite Absorbers. *ACS Energy Lett.* **2016**, *1* (6), 1199–1205. <https://doi.org/10.1021/acsenerylett.6b00495>.
  - (13) Braly, I. L.; Stoddard, R. J.; Rajagopal, A.; Uhl, A. R.; Katahara, J. K.; Jen, A. K. Y.; Hillhouse, H. W. Current-Induced Phase Segregation in Mixed Halide Hybrid Perovskites and Its Impact on Two-Terminal Tandem Solar Cell Design. *ACS Energy Lett.* **2017**, *2* (8), 1841–1847. <https://doi.org/10.1021/acsenerylett.7b00525>.
  - (14) Zhai, Y.; Wang, K.; Zhang, F.; Xiao, C.; Rose, A. H.; Zhu, K.; Beard, M. C. Individual Electron and Hole Mobilities in Lead-Halide Perovskites Revealed by Noncontact Methods. *ACS Energy Lett.* **2020**, *5* (1), 47–55. <https://doi.org/10.1021/acsenerylett.9b02310>.
  - (15) Chen, F.; Zhu, C.; Xu, C.; Fan, P.; Qin, F.; Gowri Manohari, A.; Lu, J.; Shi, Z.; Xu, Q.; Pan, A. Crystal Structure and Electron Transition Underlying Photoluminescence of



- Methylammonium Lead Bromide Perovskites. *J. Mater. Chem. C* **2017**, 5 (31), 7739–7745.  
<https://doi.org/10.1039/c7tc01945a>.
- (16) Beal, R. E.; Hagström, N. Z.; Barrier, J.; Gold-Parker, A.; Prasanna, R.; Bush, K. A.; Passarello, D.; Schelhas, L. T.; Brüning, K.; Tassone, C. J.; Steinrück, H. G.; McGehee, M. D.; Toney, M. F.; Nogueira, A. F. Structural Origins of Light-Induced Phase Segregation in Organic-Inorganic Halide Perovskite Photovoltaic Materials. *Matter* **2020**, 2 (1), 207–219.  
<https://doi.org/10.1016/j.matt.2019.11.001>.
- (17) Duong, T.; Mulmudi, H. K.; Wu, Y.; Fu, X.; Shen, H.; Peng, J.; Wu, N.; Nguyen, H. T.; Macdonald, D.; Lockrey, M.; White, T. P.; Weber, K.; Catchpole, K. Light and Electrically Induced Phase Segregation and Its Impact on the Stability of Quadruple Cation High Bandgap Perovskite Solar Cells. *ACS Appl. Mater. Interfaces* **2017**, 9 (32), 26859–26866.  
<https://doi.org/10.1021/acsami.7b06816>.
- (18) Draguta, S.; Sharia, O.; Yoon, S. J.; Brennan, M. C.; Morozov, Y. V.; Manser, J. M.; Kamat, P. V.; Schneider, W. F.; Kuno, M. Rationalizing the Light-Induced Phase Separation of Mixed Halide Organic-Inorganic Perovskites. *Nat. Commun.* **2017**, 8 (1).  
<https://doi.org/10.1038/s41467-017-00284-2>.
- (19) Yoon, S. J.; Draguta, S.; Manser, J. S.; Sharia, O.; Schneider, W. F.; Kuno, M.; Kamat, P. V. Tracking Iodide and Bromide Ion Segregation in Mixed Halide Lead Perovskites during Photoirradiation. *ACS Energy Lett.* **2016**, 1 (1), 290–296.  
<https://doi.org/10.1021/acsenergylett.6b00158>.
- (20) Yoon, S. J.; Kuno, M.; Kamat, P. V. Shift Happens. How Halide Ion Defects Influence Photoinduced Segregation in Mixed Halide Perovskites. *ACS Energy Lett.* **2017**, 2 (7), 1507–1514. <https://doi.org/10.1021/acsenergylett.7b00357>.

- (21) Barker, A. J.; Sadhanala, A.; Deschler, F.; Gandini, M.; Senanayak, S. P.; Pearce, P. M.; Mosconi, E.; Pearson, A. J.; Wu, Y.; Srimath Kandada, A. R.; Leijtens, T.; De Angelis, F.; Dutton, S. E.; Petrozza, A.; Friend, R. H. Defect-Assisted Photoinduced Halide Segregation in Mixed-Halide Perovskite Thin Films. *ACS Energy Lett.* **2017**, *2* (6), 1416–1424. <https://doi.org/10.1021/acsenergylett.7b00282>.
- (22) Cho, J.; Kamat, P. V. How Chloride Suppresses Photoinduced Phase Segregation in Mixed Halide Perovskites. *Chem. Mater.* **2020**, *32* (14), 6206–6212. <https://doi.org/10.1021/acs.chemmater.0c02100>.
- (23) Fan, W.; Shi, Y.; Shi, T.; Chu, S.; Chen, W.; Ighodalo, K. O.; Zhao, J.; Li, X.; Xiao, Z. Suppression and Reversion of Light-Induced Phase Separation in Mixed-Halide Perovskites by Oxygen Passivation. *ACS Energy Lett.* **2019**, *4* (9), 2052–2058. <https://doi.org/10.1021/acsenergylett.9b01383>.
- (24) Nandal, V.; Nair, P. R. Predictive Modeling of Ion Migration Induced Degradation in Perovskite Solar Cells. *ACS Nano* **2017**, *11* (11), 11505–11512. <https://doi.org/10.1021/acs.nano.7b06294>.
- (25) Jena, A. K.; Kulkarni, A.; Miyasaka, T. Halide Perovskite Photovoltaics: Background, Status, and Future Prospects. *Chem. Rev.* **2019**, *119* (5), 3036–3103. <https://doi.org/10.1021/acs.chemrev.8b00539>.
- (26) Shockley, W.; Queisser, H. J. Detailed Balance Limit of Efficiency of P-n Junction Solar Cells. *J. Appl. Phys.* **1961**, *32* (3), 510–519. <https://doi.org/10.1063/1.1736034>.
- (27) Agarwal, S.; Nair, P. R. Performance Loss Analysis and Design Space Optimization of Perovskite Solar Cells. *J. Appl. Phys.* **2018**, *124* (18). <https://doi.org/10.1063/1.5047841>.
- (28) Kang, H.; Kim, K. H.; Kang, T. E.; Cho, C. H.; Park, S.; Yoon, S. C.; Kim, B. J. Effect of

- Fullerene Tris-Adducts on the Photovoltaic Performance of P3HT:Fullerene Ternary Blends. *ACS Appl. Mater. Interfaces* **2013**, 5 (10), 4401–4408. <https://doi.org/10.1021/am400695e>.
- (29) Khlyabich, P. P.; Burkhart, B.; Thompson, B. C. Efficient Ternary Blend Bulk Heterojunction Solar Cells with Tunable Open-Circuit Voltage. *J. Am. Chem. Soc.* **2011**, 133 (37), 14534–14537. <https://doi.org/10.1021/ja205977z>.
- (30) Stauffer, D.; Aharony, A. *Introduction To Percolation Theory*; Taylor & Francis: London, 2018. <https://doi.org/10.1201/9781315274386>.
- (31) Synopsys. Sentaurus Device Simulation Tool. 2011.
- (32) Brennan, M. C.; Draguta, S.; Kamat, P. V.; Kuno, M. Light-Induced Anion Phase Segregation in Mixed Halide Perovskites. *ACS Energy Lett.* **2018**, 3 (1), 204–213. <https://doi.org/10.1021/acsenenergylett.7b01151>.
- (33) Lee, J. W.; Kim, S. G.; Yang, J. M.; Yang, Y.; Park, N. G. Verification and Mitigation of Ion Migration in Perovskite Solar Cells. *APL Mater.* **2019**, 7 (4). <https://doi.org/10.1063/1.5085643>.
- (34) Eames, C.; Frost, J. M.; Barnes, P. R. F.; O'Regan, B. C.; Walsh, A.; Islam, M. S. Ionic Transport in Hybrid Lead Iodide Perovskite Solar Cells. *Nat. Commun.* **2015**, 6 (May), 2–9. <https://doi.org/10.1038/ncomms8497>.
- (35) Mahesh, S.; Ball, J. M.; Oliver, R. D. J.; McMeekin, D. P.; Nayak, P. K.; Johnston, M. B.; Snaith, H. J. Revealing the Origin of Voltage Loss in Mixed-Halide Perovskite Solar Cells. *Energy Environ. Sci.* **2020**, 13 (1), 258–267. <https://doi.org/10.1039/c9ee02162k>.
- (36) Yang, Z.; Rajagopal, A.; Jo, S. B.; Chueh, C. C.; Williams, S.; Huang, C. C.; Katahara, J. K.; Hillhouse, H. W.; Jen, A. K. Y. Stabilized Wide Bandgap Perovskite Solar Cells by Tin

- Substitution. *Nano Lett.* **2016**, *16* (12), 7739–7747.  
<https://doi.org/10.1021/acs.nanolett.6b03857>.
- (37) Bischak, C. G.; Hetherington, C. L.; Wu, H.; Aloni, S.; Ogletree, D. F.; Limmer, D. T.; Ginsberg, N. S. Origin of Reversible Photoinduced Phase Separation in Hybrid Perovskites. *Nano Lett.* **2017**, *17* (2), 1028–1033. <https://doi.org/10.1021/acs.nanolett.6b04453>.
- (38) Elmelund, T.; Seger, B.; Kuno, M.; Kamat, P. V. How Interplay between Photo and Thermal Activation Dictates Halide Ion Segregation in Mixed Halide Perovskites. *ACS Energy Lett.* **2020**, *5* (1), 56–63. <https://doi.org/10.1021/acsenergylett.9b02265>.
- (39) Brennan, M. C.; Draguta, S.; Kamat, P. V.; Kuno, M. Light-Induced Anion Phase Segregation in Mixed Halide Perovskites. *ACS Energy Lett.* **2018**, *3* (1), 204–213. <https://doi.org/10.1021/acsenergylett.7b01151>.
- (40) Samu, G. F.; Janáky, C.; Kamat, P. V. A Victim of Halide Ion Segregation. How Light Soaking Affects Solar Cell Performance of Mixed Halide Lead Perovskites. *ACS Energy Lett.* **2017**, *2* (8), 1860–1861. <https://doi.org/10.1021/acsenergylett.7b00589>.
- (41) Yang, X.; Yan, X.; Wang, W.; Zhu, X.; Li, H.; Ma, W.; Sheng, C. X. Light Induced Metastable Modification of Optical Properties in CH<sub>3</sub>NH<sub>3</sub>PbI<sub>3</sub>-XBr<sub>x</sub> Perovskite Films: Two-Step Mechanism. *Org. Electron. physics, Mater. Appl.* **2016**, *34*, 79–83. <https://doi.org/10.1016/j.orgel.2016.04.020>.
- (42) Hu, M.; Bi, C.; Yuan, Y.; Bai, Y.; Huang, J. Stabilized Wide Bandgap MAPbBr<sub>x</sub>I<sub>3-x</sub> Perovskite by Enhanced Grain Size and Improved Crystallinity. *Adv. Sci.* **2015**, *3* (6), 6–11. <https://doi.org/10.1002/advs.201500301>.
- (43) Knight, A. J.; Herz, L. M. Preventing Phase Segregation in Mixed-Halide Perovskites: A Perspective. *Energy Environ. Sci.* **2020**, 2024–2046. <https://doi.org/10.1039/d0ee00788a>.